

H4K20me3 upregulated by reactive oxygen species is associated with tumor progression and poor prognosis in patients with hepatocellular carcinoma

Suchittra Phoyen^a, Anapat Sanpavat^b, Chakriwong Ma-on^c, Ulrike Stein^{d,e}, Nattiya Hirankarn^f, Pisit Tangkijvanich^{a,g}, Depicha Jindatip^h, Patcharawalai Whongsiriⁱ, Chanchai Boonla^{a,*}

^a Department of Biochemistry, Faculty of Medicine, Chulalongkorn University, Bangkok, Thailand

^b Department of Pathology, Faculty of Medicine, Chulalongkorn University, Bangkok, Thailand

^c Department of Pathology, Faculty of Medicine Siriraj Hospital, Mahidol University, Bangkok, Thailand

^d Translational Oncology of Solid Tumors, Experimental and Clinical Research Center, Charité Universitätsmedizin Berlin and Max-Delbrück-Center for Molecular Medicine, Berlin, Germany

^e German Cancer Consortium, Heidelberg, Germany

^f Center of Excellence in Immunology and Immune-Mediated Diseases, Department of Microbiology, Faculty of Medicine, Chulalongkorn University, Bangkok, Thailand

^g Center of Excellence in Hepatitis and Liver Cancer, Faculty of Medicine, Chulalongkorn University, Bangkok, Thailand

^h Department of Anatomy, Faculty of Medicine, Chulalongkorn University, Bangkok, Thailand

ⁱ Department of Biochemistry and Microbiology, Faculty of Pharmaceutical Sciences, Chulalongkorn University, Bangkok, Thailand

ARTICLE INFO

Keywords:

H4K20me3
Histone methylation
Oxidative stress
Hepatocellular carcinoma
Prognosis

ABSTRACT

Epigenetic alteration by oxidative stress is vitally involved in carcinogenesis and cancer progression. Previously, we demonstrated that oxidative stress was increased in hepatocellular carcinoma (HCC) patients and associated with tumor aggressiveness. Herein, we immunohistochemically investigated whether histone methylation, specifically H4K20me3, was upregulated in human hepatic tissues obtained from HCC patients (n = 100). Also, we experimentally explored if the H4K20me3 was upregulated by reactive oxygen species (ROS) and contributed to tumor progression in HCC cell lines. We found that H4K20me3 level was increased in HCC tissues compared with the adjacent noncancerous liver tissues. H3K9me3 and H3K4me3 levels were also increased in HCC tissues. Cox regression analysis revealed that the elevated H4K20me3 level was associated with tumor recurrence and short survival in HCC patients. Experimentally, H₂O₂ provoked oxidative stress and induced H4K20me3 formation in HepG2 and Huh7 cells. Transcript expression of histone methyltransferase Suv420h2 (for H4K20me3), Suv39h1 (for H3K9me3), and Smdy3 (for H3K4me3) were upregulated in H₂O₂-treated HCC cells. H₂O₂ also induced epithelial-mesenchymal transition (EMT) in HCC cells, indicated by decreased E-cadherin but increased α -SMA and MMP-9 mRNA expression. Migration, invasion, and colony formation in HCC cells were markedly increased following the H₂O₂ exposure. Inhibition of H4K20me3 formation by A196 (a selective inhibitor of Suv420h2) attenuated EMT and reduced tumor migration in H₂O₂-treated HCC cells. In conclusion, we demonstrated for the first time that H4K20me3 level was increased in human HCC tissues, and it was independently associated with

* Corresponding author. Department of Biochemistry, Faculty of Medicine, Chulalongkorn University, Rama IV Rd, Bangkok, 10330, Thailand. E-mail address: chanchai.b@chula.ac.th (C. Boonla).

<https://doi.org/10.1016/j.heliyon.2023.e22589>

Received 30 January 2023; Received in revised form 13 November 2023; Accepted 15 November 2023

Available online 20 November 2023

2405-8440/© 2023 Published by Elsevier Ltd.

This is an open access article under the CC BY-NC-ND license

(<http://creativecommons.org/licenses/by-nc-nd/4.0/>).

poor prognosis in HCC patients. ROS upregulated H4K20me3 formation, induced mRNA expression of EMT markers, and promoted tumor progression in human HCC cells. Inhibition of H4K20me3 formation reduced EMT and tumor aggressive phenotypes in ROS-treated HCC cells. Possibly, ROS-induced EMT and tumor progression in HCC cells was epigenetically mediated through an increased formation of repressive chromatin H4K20me3.

1. Introduction

Alteration of histone methylation changes gene expression and contributes to the development of several diseases, including cancer. The most well-characterized chromatin marks for inactive chromatin and gene silencing are H3K9me3, H3K27me3, and H4K20me3, whereas the best-known mark for active chromatin and transcriptional activation is H3K4me3. Alteration of these chromatin marks is contributed to tumorigenesis and progression of human cancers [1]. In hepatocellular carcinoma (HCC), dysregulation of H3K4me3, H3K9me3, and H3K27me3 are well recognized [2], but the formation and oncogenic contribution of H4K20me3 in HCC are only slightly explored.

Mechanistically, development of HCC is linked to oxidative stress [3–6] and dysregulated histone methylation [2]. We previously reported an increased oxidative stress in HCC patients compared with healthy subjects [5]. Furthermore, we demonstrated that Nrf2 and 8-hydroxydeoxyguanosine (8-OHdG) were upregulated in HCC tissues of the patients [3]. According to the literature, H3K4me3 and its lysine methyltransferase (Smyd3) are upregulated in human HCC tissues, and elevated level of H3K4me3 was associated with poor survival in HCC patients [7]. Increased H3K9me3 level is also demonstrated in human HCC tissues, and it is correlated with the tumor differentiation [8]. For H3K27me3, its level is also increased in human HCC tissues [9,10]. Still, formation and clinical significance of H4K20me3 repressive chromatin mark in human HCC have not been investigated.

Oxidative stress induced by reactive oxygen species (ROS) has been demonstrated to alter histone modification pattern [11,12]. Increased histone H4 acetylation was demonstrated in alveolar epithelial A549 cells exposed to H₂O₂ [13]. Chronic exposure of human kidney cells to H₂O₂ caused downregulation of H3K4ac and H3K9ac, but upregulation of H3K4me3 and H3K27me3 [14]. Hitherto, a cause-and-effect relationship between ROS and H4K20me3 formation in HCC has not been explored.

In this study, we investigated the level of H4K20me3 in liver tissues obtained from Thai HCC patients using immunohistochemical staining. Levels of H3K9me3 and H3K4me3 in HCC tissues were also immunohistochemically explored. Association of H4K20me3 level with tumor recurrence and patients' survival were evaluated. Furthermore, we experimentally investigated whether ROS could increase levels of these three chromatin marks, particularly H4K20me3, and promote HCC progression.

Table 1
Demographic and clinical data of the HCC patients.

Characteristics	Frequency (%)
Number of patients	92
Age (mean ± SD) (year old)	64.0 ± 11.0
Sex	
• Male	79 (86.0 %)
• Female	13 (14.0 %)
Hepatitis B infection	51 (55.4 %)
Hepatitis C infection	12 (13.0 %)
Alcoholic disease	6 (6.5 %)
Nonalcoholic steatohepatitis (NASH)	2 (2.2 %)
Tumor differentiation	
• Well differentiation	27 (29.3 %)
• Moderate differentiation	49 (53.2 %)
• Poor differentiation	16 (17.4 %)
Cirrhosis (n = 75)	
• Yes	46 (61.3 %)
• No	29 (38.7 %)
Metastasis (n = 74)	
• Yes	5 (6.8 %)
• No	69 (93.2 %)
Total bilirubin (mean ± SD, mg/dL)	1.9 ± 4.4
Albumin (mean ± SD, mg/dL)	3.4 ± 0.7
SGOT (mean ± SD, U/L)	357.4 ± 603.9
SGPT (mean ± SD, U/L)	269.8 ± 416.7
ALP (mean ± SD, U/L)	94.0 ± 81.1

2. Materials and methods

2.1. Patients and paraffin-embedded tissues

Immunohistochemical (IHC) staining for H4K20me3 was performed in 100 paraffin-embedded liver sections obtained from histologically proved HCC patients. Of 100, 92 cases (mean aged 64 ± 11 years, 79 (86 %) males and 13 (14 %) females) had clinical data available for association analysis. Demographic and clinical data of studied HCC patients are displayed in [Table 1](#). Levels of H3K9me3 and H3K4me3 in human HCC tissues were previously reported in many studies [7,8]. Therefore, in this study, the IHC staining for H3K9me3 and H3K4me3 was carried out only in 32 and 31 HCC sections, respectively, to confirm whether their levels in our HCC cohorts were similar to that previously reported. In all 100 HCC liver sections, 15 sections contained both cancerous and adjacent noncancerous areas and were called paired tissue sections.

2.2. Immunohistochemical staining

Paraffin-embedded sections were deparaffinized and rehydrated. Heat-induced antigen retrieval was performed in sodium citrate buffer (pH 6.0). Endogenous peroxidase was inactivated by incubating in 0.3 % H₂O₂ solution for 30 min. Non-specific binding was blocked with normal horse serum (RTU Vectastain Kit, PK-7200) for 30 min. Sections were incubated with primary antibodies either 1:250 H4K20me3 (ab9053, Abcam), or 1:500 H3K9me3 (ab8898, Abcam), or 1:500 H3K4me3 (ab8580, Abcam) at 4 °C, overnight. After washing, sections were incubated with the biotinylated universal antibody for 1 h, followed by ABC reagent for 30 min (Universal Elite Vector Kit, PK-7200). Immunoreactive complexes were visualized using diaminobenzidine (DAB) staining. Sections were counterstained with hematoxylin. Finally, the stained sections were dehydrated, cleared, and mounted.

Relative levels of H4K20me3, H3K9me3, and H3K4me3 formation were evaluated based on the percentage of positive hepatocytes (graded into 0 = 0 %, 1 = 1–25 %, 2 = 26–50 %, 3 = 51–75 %, 4 = 75–100 %) and the intensity of staining (quantified by the Celleste Image Analysis Software, Thermo Fisher Scientific: intensity level >150–180 = 0, >120–150 = 1, >90–120 = 2, >60–90 = 3, 30–60 = 4), averaged from five different microscopic fields. IHC score was calculated by multiplication of % positive cell score (0–4) with intensity score (0–4). Therefore, the minimum IHC score was 0, and the maximum was 16. Representative micrographs for IHC scores of 8, 12, and 16 are shown in [Supplementary Fig. 1](#).

2.3. HCC cell lines and cultured condition

Two HCC cell lines, HepG2 (kindly gift from Prof. Antonio Bertoleti, Singapore Institute for Clinical Sciences, A*Star) and Huh7 (JCRB0403, Osaka, Japan), were used in the study. Cells were maintained in DMEM/high glucose medium without pyruvate (Hyclone) containing FBS and non-essential amino acid in a 5 % CO₂ incubator at 37 °C. Oxidative stress in HCC cells was induced by exposure to the sub-lethal concentrations of H₂O₂ (30 μM for HepG2 and 60 μM for Huh7; appropriate concentrations that could induce the highest degree of oxidative stress in cells with a minimum cytotoxicity) for 72 h in serum-free medium. Based on the MTT assay, H₂O₂ concentrations of 30 μM and 60 μM showed the minimal cytotoxic effect to HepG2 and Huh7 cells, respectively ([Supplementary Fig. 2](#)). Therefore, we opted to use these concentrations in the subsequent experiments. The treatment period of 72 h was selected because it caused an apparent increase in tumor progressive activities in HCC cells following the H₂O₂ treatment.

2.4. Intracellular ROS generation

Dichloro-dihydro-fluorescein diacetate (DCFH-DA) assay was employed to determine ROS production in HCC cells [15]. Cells were seeded in 96-well black plate and incubated at 37 °C with 5 % CO₂ overnight, and then incubated with the freshly prepared DCFH-DA solution (0.5 mM in serum-free DMEM) at 37 °C for 30 min. After washing with PBS, a conditioned medium containing H₂O₂ was added to each well. Fluorescent intensity was measured (excitation at 480 nm, emission at 535 nm) at the beginning (T₀) and at the end at 60 min (T₆₀). The arbitrary fluorescent unit (AFU) indicated the level of intracellular ROS was calculated from T₆₀/T₀.

2.5. Protein carbonylation assay

After 72 h of treatment, cells were lysed using radioimmunoprecipitation assay (RIPA) buffer containing protease inhibitor cocktail. Protein concentration was determined by bicinchoninic acid assay. Protein carbonyl content was measured as described earlier [15]. Cell lysates were incubated with 10 mM DNPH (test) or 2 N HCl (reagent blank) for 60 min in the dark. Cold 20 % trichloroacetic acid was added and incubated on ice for 10 min. After centrifugation (10,000×g, 4 °C for 15 min), the pellet was collected and washed with ethanol: ethyl acetate (1:1 vol ratio), then centrifugated at 10,000×g, 4 °C for 30 min. The washed pellet was then dissolved in 6 M guanidine chloride at 60 °C for 30 min. Absorbance at 375 nm was measured. The level of protein carbonyl normalized by total protein content was calculated from ((A₃₄₇^{DNPH}-A₃₇₅^{HCl}) × 45.45)/protein concentration.

2.6. Total antioxidant capacity (TAC) measurement

TAC was measured using the 2, 2-diphenyl-1-picrylhydrazyl (DPPH) method. DPPH was freshly prepared in 80 % methanol. Absorbance (at 517 nm) of the DPPH solution was adjusted to 0.650 ± 0.020 before use. Sample (test) or water (blank) (5 μL) was

added to the DPPH solution (295 μ L). The mixture was incubated at room temperature for 30 min in the dark, and absorbance (A) at 517 nm was measured. Antioxidant activity (%AA) of each sample was calculated from: %AA = $((A_{\text{blank}} - A_{\text{test}}) / A_{\text{blank}}) \times 100$. Vitamin C standard with known concentrations (0, 0.25, 0.5, and 1 mM) was used to generate a standard curve (%AA vs. vitamin C concentrations). TAC of each sample was derived from the standard curve and expressed as vitamin C equivalent antioxidant capacity (VCEAC).

2.7. RNA extraction and quantitative reverse transcription-polymerase chain reaction (qRT-PCR)

Total RNA was extracted from HCC cells using the GF-1 total RNA extraction kit (Vivantis, Buckinghamshire, Malaysia), and RNA concentration was measured using a Nanodrop spectrophotometer (Thermo Scientific, Wilmington, USA). cDNA was synthesized from RNA template (1 μ g) using the reverse transcription kit (Thermo Scientific, USA). The qPCR was performed in the QuantStudio™ 6 Real-Time PCR system (Thermo Fisher Scientific) using SYBR Green PCR Master Mix (Biotecrabbt, Germany) and specific primers (Supplementary Table 1). Relative mRNA expression was calculated by the $2^{-\Delta\Delta CT}$ method normalized against GAPDH endogenous control. Experiments were done in triplicate.

2.8. Western blot

Histone protein samples were separated by SDS-PAGE (12 % gel). After electrophoresis (100 V for 20 min, and 200 V for 30 min), proteins were transferred to a PVDF membrane (180 mA for 60 min). Membrane was incubated with 5 % skimmed milk in TBS-T at room temperature for 1 h, followed by primary antibodies either 1:10,000 H4K20me3 (ab9053, Abcam) or 1:20,000 H3K9me3 (ab8898, Abcam) or 1:20,000 H3K4me3 (ab8580, Abcam) antibodies at 4 °C overnight. After washing, membrane was incubated with 1:10,000 corresponding secondary antibodies for 1 h. The immunocomplex signal was developed using the SuperSignal™ West Femto Maximum Sensitivity Substrate (ThermoFisher Scientific) and imaged using the ChemiDoc™ Touch Imaging System (Bio-Rad Laboratories). Histone H4 and Histone H3 were detected as loading controls using 1:10,000 anti-Histone H4 mouse antibodies (mAbcam 31830, Abcam) and 1:20,000 anti-Histone H3 mouse antibodies (14269, Cell Signaling Technology), respectively. Experiments were done in triplicate.

2.9. Transwell assay for cell migration

After treating with or without H₂O₂ for 72 h, cells (5×10^4 cells in serum-free DMEM) were seeded in a Transwell chamber (pore size of 8 μ m). Fresh medium containing 10 % FBS was added to the bottom chamber. After 24 h incubation, cells that migrated to the lower chamber were trypsinized and transferred to the medium with FBS. Resuspended cells were incubated with the CellTiter-Glo® (Promega) and shaken for 10 min at room temperature. Luciferase activity reflecting numbers of migrated cells was measured (Tecan infinite 200 PRO). Experiments were done in triplicate.

2.10. Boyden chamber assay for cell invasion

Matrigel-precoated Transwell chambers (8 μ m pore size, BD Falcon, USA) were rehydrated in DMEM for 2 h at 37 °C. Cells resuspended in serum-free DMEM were added to the upper chamber (insert). DMEM supplemented with 10 % FBS was added to the lower chamber. After 24 h incubation, non-invaded cells in the upper chamber were removed using a cotton-tipped swab. Invaded cells were stained with crystal violet and counted under the light microscope. Experiments were done in triplicate.

2.11. Clonogenic assay

After 72 h treatment, approximately 1×10^3 cells in DMEM containing 10 % FBS were seeded in a 6-well plate. Colonies were grown for 7–14 days. Cells were fixed and stained with the FixNStain solution containing 4 % formaldehyde and 0.1 % crystal violet for 10 min. Then, cells were washed with tap water and dried at room temperature. The number of colonies was counted and imaged using the AlphaView Stand Alone ver. 1.2 Software. Experiments were done in triplicate.

2.12. Statistical analysis

Data were presented as mean \pm standard error of mean (SEM). Categorical data were presented as frequency and percentage. Two-sample *t*-test or Mann-Whitney test was used to find the difference between the two independent groups. The difference in paired tissue samples was tested by paired sample *t*-test. Kaplan–Meier (KM) survival curve was created. The equality of KM curves was tested using a log-rank test. Cox regression was used to calculate the hazard ratio (HR). GraphPad Prism 9.5.1 (GraphPad, La Jolla, CA) and StataSE 12 (StataCrop LLC, College Station, TX) were employed for graphs and statistical analyses. *P* value < 0.05 was considered statistically significant.

3. Results

3.1. Increased levels of H4K20me3, H3K9me3, and H3K4me3 in human HCC tissues

Level of H4K20me3, labeled in the nuclei of hepatocytes, was increased in HCC tissues compared with the adjacent noncancerous liver tissues (Fig. 1A). IHC score of H4K20me3 in HCC tissues (n = 100) was significantly higher than that in noncancerous tissues (n = 15) (P = 0.0004). In 15 HCC sections that contained both cancerous and noncancerous areas (paired cancerous and noncancerous liver tissues), the level of H4K20me3 in cancerous tissues was significantly greater than in noncancerous tissues (P = 0.001) (Fig. 1A). The H3K9me3 level in HCC tissues was increased compared with the noncancerous tissues (Fig. 1B). The IHC score of H3K9me3 in HCC tissues (n = 32) was significantly higher than noncancerous tissues (n = 15) (P < 0.0001). Also, the level of H3K4me3 was increased in HCC tissues relative to the noncancerous tissues (Fig. 1C). The IHC score of H3K4me3 in HCC tissues (n = 31) was significantly higher than in noncancerous tissues (n = 15) (P < 0.0001). In the paired hepatic sections containing both cancerous and noncancerous areas, IHC scores of both H3K9me3 and H3K4me3 were significantly higher in cancerous areas than in noncancerous areas. Both H3K9me3 and H3K4me3 were clearly stained in nuclei of hepatocytes.

H&E staining was performed in all tissue sections, and the stained sections were evaluated by the pathologist (A.S.) to denote the cancerous and noncancerous areas. Representative H&E-stained liver tissues were displayed in Supplementary Fig. 3.

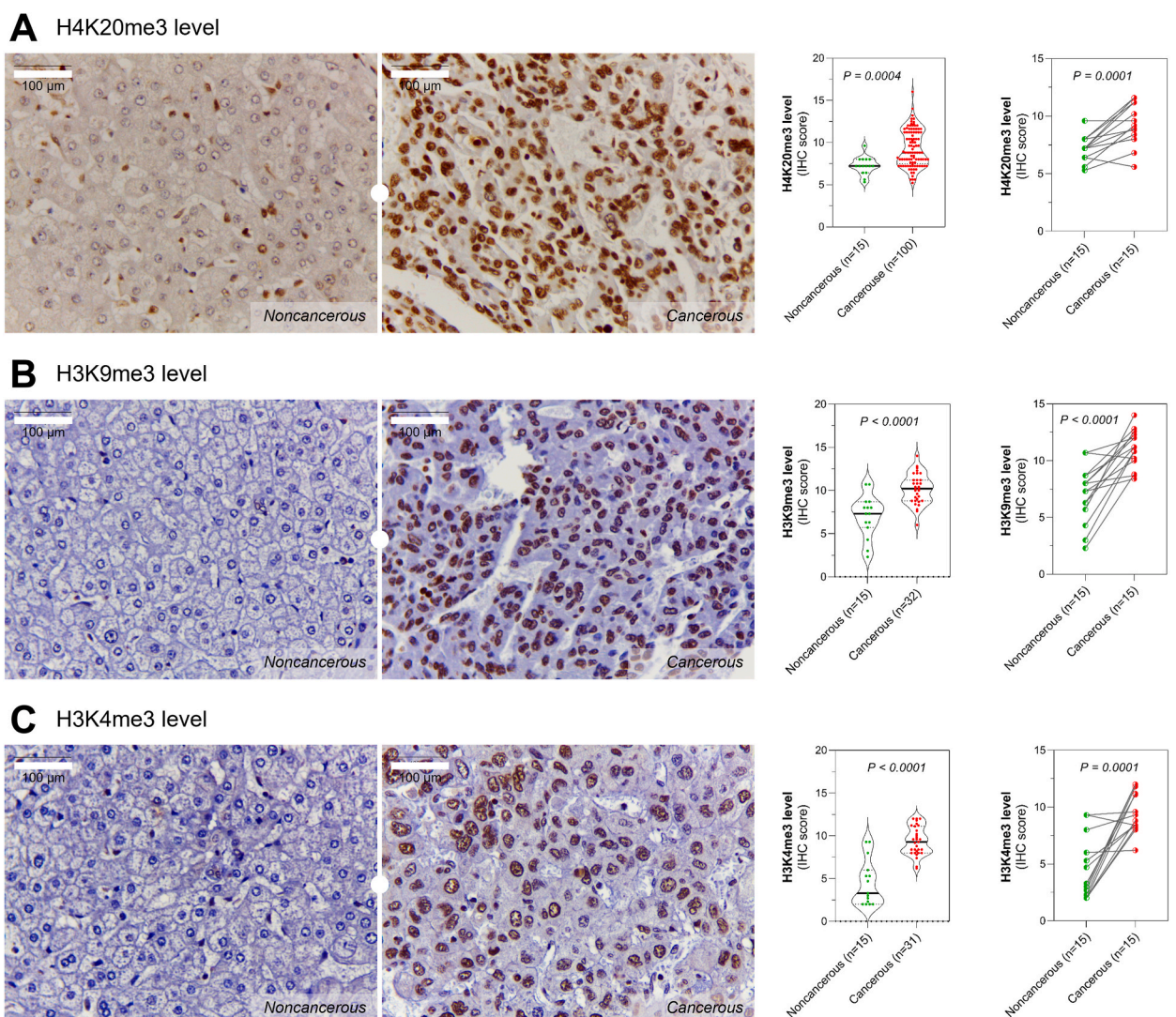


Fig. 1. IHC staining of H4K20me3, H3K9me3 and H3K4me3 in human HCC tissues. A: Representative micrographs of H4K20me3 compared between noncancerous and cancerous hepatic tissues. B: Representative micrographs of H3K9me3 compared between noncancerous and cancerous hepatic tissues. C: Representative micrographs of H3K4me3 compared between noncancerous and cancerous hepatic tissues. Bars in micrographs: 100 μm. Magnification: 400×.

3.2. Elevated level of H4K20me3 associated with poor prognosis

Associations of H4K20me3 level with time to tumor recurrence and patients' survival were evaluated using the KM curve estimator. Level of H4K20me3 formation was categorized into two groups, high (IHC score ≥ 7.3 , $n = 55$) and low (IHC score < 7.3 , $n = 18$) levels. High level of H4K20me3 was associated with tumor recurrence (Fig. 2A). The log-rank test revealed that high H4K20me3 level was significantly associated with an increased risk of tumor recurrence ($P = 0.0259$). Based on Cox regression analysis, patients with high H4K20me3 level had 3.77 times higher risk for tumor recurrence than those with low H4K20me3 level (crude HR: 3.77, 95 % CI: 1.09–13.11). After adjusting for age, sex, and tumor differentiation, the adjusted HR of 3.72 (95 % CI: 1.07–12.96) was obtained.

Association of H4K20me3 level with overall survival of HCC patients was further evaluated. Hepatic level of H4K20me3 was recategorized into elevated (IHC score ≥ 11 , $n = 27$) and low (IHC score < 11 , $n = 65$) levels. Elevated H4K20me3 was significantly associated with a short survival in HCC patients (Log-rank test $P = 0.0306$) with crude HR of 2.78 (95 % CI: 1.06–7.30) (Fig. 2B). After adjusting for age, sex, and tumor differentiation, the adjusted HR of 4.00 (95 % CI: 1.21–13.26) was revealed, indicated that patients with elevated H4K20me3 level had 4 times higher risk of death than those with low H4K20me3 level.

Level of H4K20me3 in HCC tissues were compared among patients with different etiology. We found no significant difference of IHC score of H4K20me3 among HCC patients with hepatitis B infection, those with hepatitis C infection, those with alcoholic disease, those with NASH, and those with other causes (Supplementary Fig. 4).

3.3. H4K20me3 formation induced by ROS in HCC cells

HepG2 and Huh7 cells exposed to H_2O_2 (at sub-toxic concentrations) had significantly increased intracellular ROS production (Fig. 3A and F) and protein carbonylation (Fig. 3B and G). By contrast, the levels of TAC in HepG2 and Huh7 cells treated with H_2O_2 were significantly lower than in the untreated controls (Fig. 3C and H). Moreover, transcript expression of Nrf2 and NQO1 were significantly upregulated in HepG2 and Huh7 cells treated with H_2O_2 compared with the untreated controls (Fig. 3D, E, 3I and 3J). These indicated that H_2O_2 -treated HCC cells were experiencing oxidative stress.

Level of H4K20me3, H3K9me3, and H3K4me3 in HCC cells was increased in H_2O_2 -treated conditions relative to untreated controls (Fig. 4A). Band intensity quantitation showed that the level of H4K20me3 following H_2O_2 treatment in both HepG2 and Huh7 cells was significantly higher than untreated control (Fig. 4B). Also, H3K4me3 level in H_2O_2 -treated Huh7 cells was significantly higher than in untreated control. Following H_2O_2 treatment, H3K9me3 level tended to be increased in both HepG2 and Huh7 cells, but H3K4me3 level tended to be increased in HepG2 cells.

Transcript expression of histone lysine methyltransferases responsible for forming H4K20me3 (Suv420h2), H3K9me3 (Suv39h1) and H3K4me3 (Smyd3) were investigated (Fig. 5). The expression of Suv39h1 mRNA was significantly upregulated in H_2O_2 -treated HCC cells (both HepG2 and Huh7) compared with untreated controls (Fig. 5B and E). Likewise, Suv420h2 and Smyd3 mRNA expression were significantly increased in H_2O_2 -treated Huh7 cells compared with controls (Fig. 5D and F), but they were marginally increased in H_2O_2 -treated HepG2 cells (Fig. 5A and C).

3.4. Tumor aggressiveness augmented by ROS in HCC cells

Several lines of evidence demonstrate that ROS induce epithelial-mesenchymal transition (EMT) and contribute to tumor progression [16,17]. In this study, we found that E-cadherin mRNA expression was significantly lower in HepG2 and Huh7 cells treated with H_2O_2 than untreated controls (Fig. 6A and D). By contrast, α -SMA mRNA expression was significantly upregulated following the H_2O_2 treatment in both HepG2 and Huh7 cells compared with untreated controls (Fig. 6B and E). In addition, expression of MMP-9 mRNA in H_2O_2 -treated cells (both HepG2 and Huh7) was significantly greater than untreated controls (Fig. 6C and F).

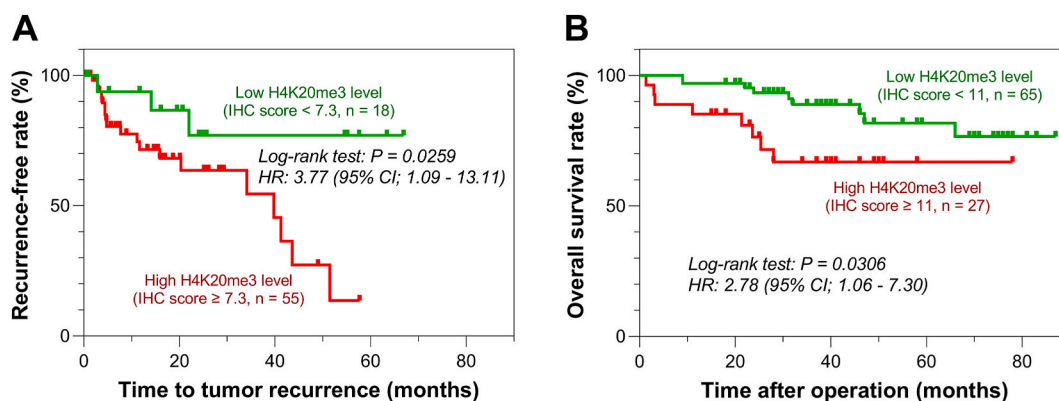
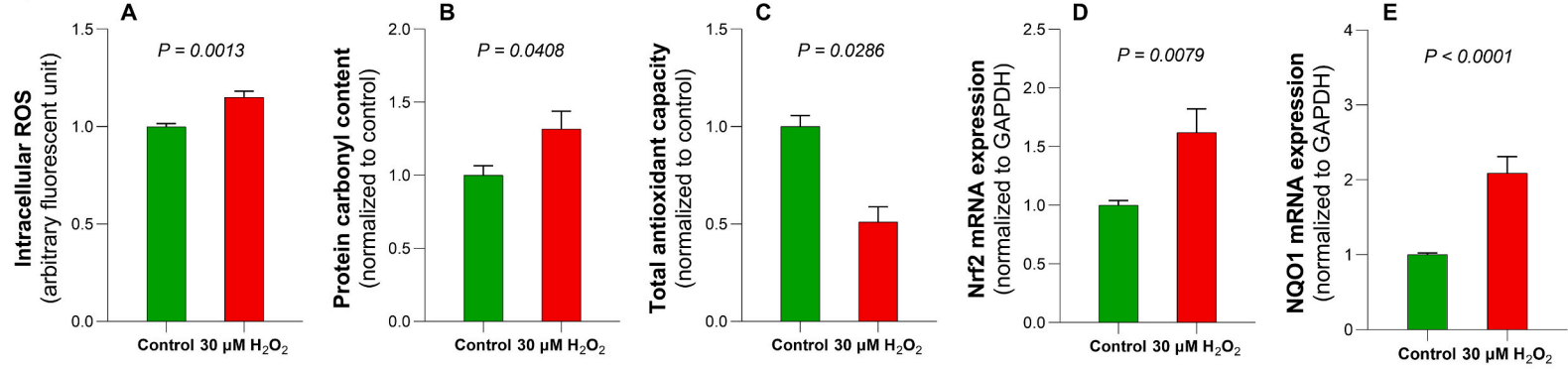


Fig. 2. Kaplan-Meier survival analysis based on H4K20me3 level in HCC patients. A: KM survival curve for tumor recurrence compared between low (green line) and high (red line) H4K20me3 level. B: KM survival curve for overall survival compared between low (green line) and high (red line) H4K20me3 level.

HepG2



Huh7

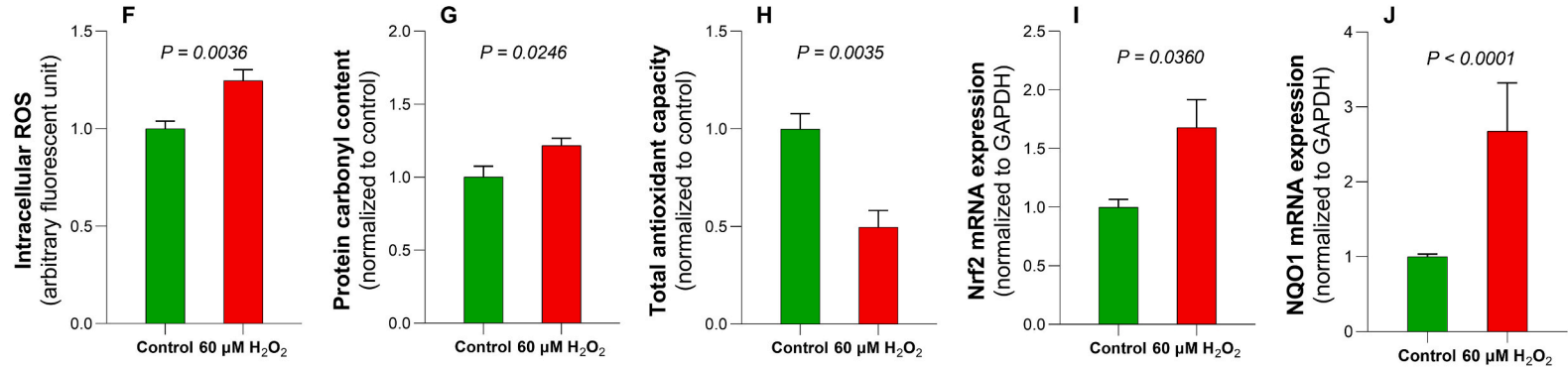


Fig. 3. Oxidative stress induction by ROS in HCC cells (72 h exposure). A: Intracellular ROS production in HepG2. B: Protein carbonyl content in HepG2. C: Total antioxidant capacity in HepG2. D: Relative Nrf2 mRNA expression in HepG2. E: Relative NQO1 mRNA expression in HepG2. F: Intracellular ROS production in Huh7. G: Protein carbonyl content in Huh7. H: Total antioxidant capacity in Huh7. I: Relative Nrf2 mRNA expression in Huh7. J: Relative NQO1 mRNA expression in Huh7. Experiments were done in triplicate. Error bars indicate SEM.

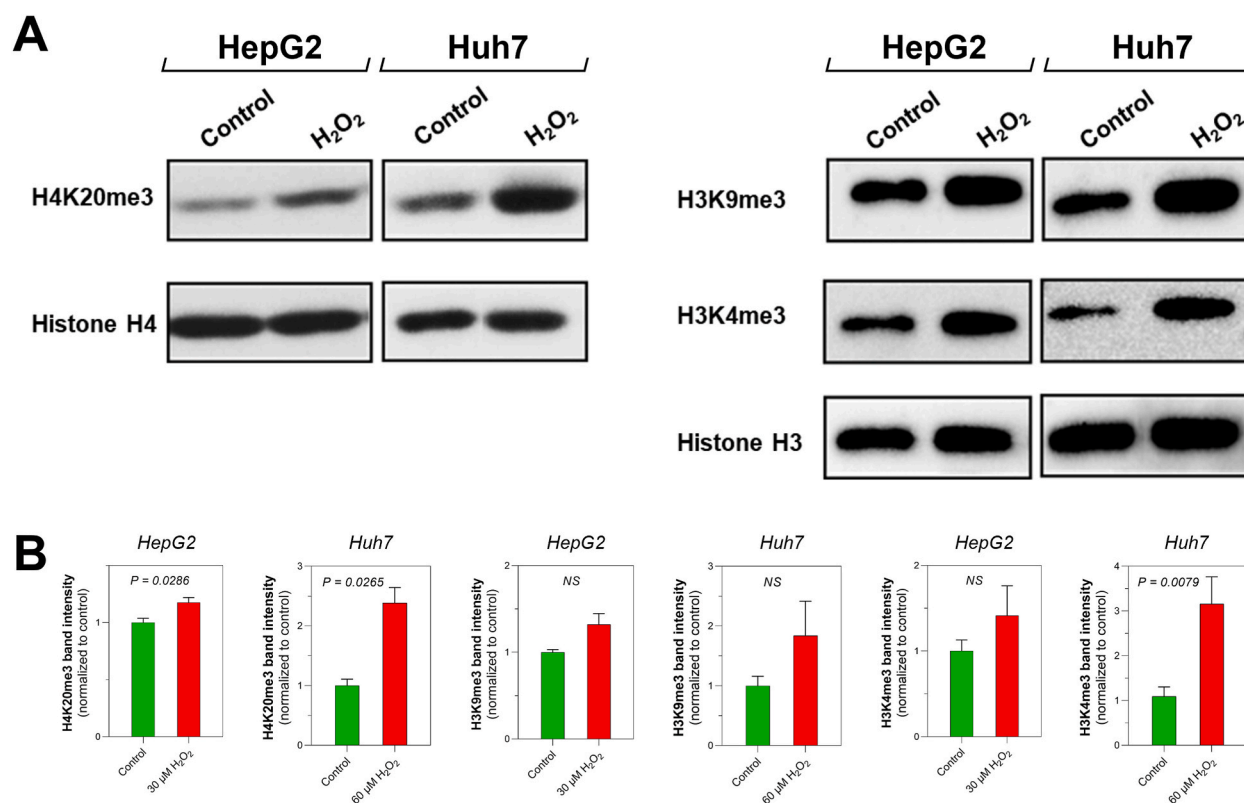


Fig. 4. Histone methylation changes by ROS in HepG2 and Huh7 cells. **A:** Western blot images of H4K20me3, H3K9me3 and H3K4me3 compared between H₂O₂-treated and untreated control conditions. Were also increased in H₂O₂ treated cells compared with untreated controls. **B:** Band intensity quantitation of H4K20me3, H3K9me3 and H3K4me3 compared between H₂O₂-treated and control conditions. Experiments were done in triplicate. Error bars indicate SEM. The full non-adjusted blot images are shown in [Supplementary Fig. 5](#).

Change in progressiveness of HCC cells following ROS treatment was determined. The number of migrated and invaded cells following H₂O₂ treatment (both for HepG2 and Huh7) were significantly higher than untreated controls ([Fig. 7A](#) and [B](#)). The colony formation assay showed that the number of colonies formed in H₂O₂-treated condition (both for HepG2 and Huh7) were significantly higher than those untreated controls ([Fig. 7C](#)). These suggested that ROS increased the progressive activity of HCC cells, at least in part, through EMT.

We further investigated whether inhibition of H4K20me3 formation could inhibit EMT and reduce tumor aggressive activity in H₂O₂-treated HCC cells. A196 was used as a selective inhibitor of Suv420 histone methyltransferases. Tocopheryl acetate (TA), as antioxidant, was used to see whether attenuation of oxidative stress could also reduce EMT and tumor aggressiveness in H₂O₂-treated HCC cells. We found that A196, but not TA, effectively reduced H4K20me3 level in H₂O₂-treated HepG2 and Huh7 cells ([Fig. 8A](#)). The mRNA expression of EMT mesenchymal marker α -SMA in H₂O₂-treated HepG2 cells was significantly reduced by both A196 and TA ([Fig. 8B](#)). Cell migration assay demonstrated that both A196 and TA significantly reduce the migration activity in H₂O₂-treated HepG2 and Huh7 cells ([Fig. 8C](#)). Therefore, the inhibition of H4K20me3 formation by A196 could reduce EMT and tumor aggressive activity in H₂O₂-treated HCC cells. Although it was not extensively investigated, our present findings suggested that ROS-induced HCC progression was, at least in part, mediated through an increased H4K20me3 formation.

4. Discussion

We investigated whether ROS altered histone methylations and promoted tumor progression in HCC. We found that formation of H4K20me3, H3K9me3, and H3K4me3 were significantly increased in human HCC tissues compared with the adjacent noncancerous liver tissues. Elevated level of H4K20me3 was independently associated with tumor recurrence and poor survival in HCC patients. Experimentally, H₂O₂ provoked oxidative stress and upregulated H4K20me3 formation in HepG2 and Huh7 cells. H₂O₂ increased mRNA expression of EMT markers and enhanced migration, invasion, and colony formation of HCC cells. Inhibition of H4K20me3 formation by Suv420 histone methyltransferase inhibitor A196 reduced EMT and migration activity in H₂O₂-treated HCC cells. Our findings suggested that the induction of EMT and tumor aggressiveness in HCC cells following ROS exposure was, at least in part, mediated through an increased H4K20me3 formation.

We clearly showed that H4K20me3 was upregulated in HCC tissues compared with the adjacent noncancerous liver tissues, and the

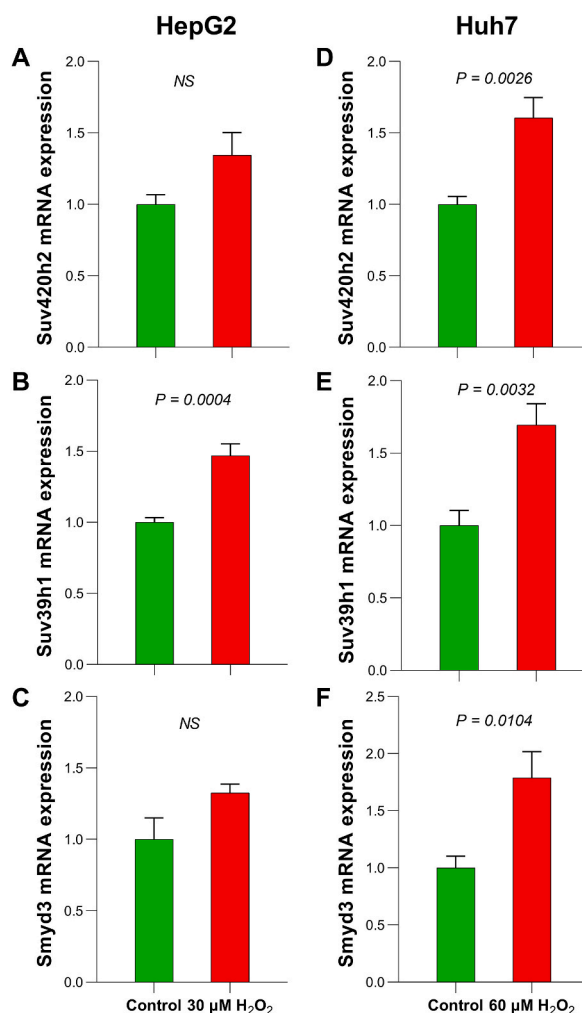


Fig. 5. Transcript levels of histone methyltransferases upregulated by ROS in HepG2 and Huh7 cells. A: Suv420h2 mRNA expression in HepG2 following H₂O₂ treatment. B: Suv39h1 mRNA expression in HepG2 following H₂O₂ treatment. C: Smyd3 mRNA expression in HepG2 following H₂O₂ treatment. D: Suv420h2 mRNA expression in Huh7 following H₂O₂ treatment. E: Suv39h1 mRNA expression in Huh7 following H₂O₂ treatment. F: Smyd3 mRNA expression in Huh7 following H₂O₂ treatment. Experiments were done in triplicate. Error bars indicate SEM.

elevated level of H4K20me3 could independently predict the tumor recurrence (adjusted HR: 3.72 (95 % CI: 1.07–12.96) and patients' survival (adjusted HR: 4.00 (95 % CI: 1.21–13.26)). These data indicated that HCC patients with elevated H4K20me3 level had about 4 times higher risks for tumor recurrence and death than those with low level. According to the literature, both upregulation and downregulation of H4K20me3 were reported in malignant tissues, for instances, upregulation in brain cancer [18], and downregulation in lung [19] and colorectal [20] cancers. Our study is the first study demonstrating that H4K20me3 level is increased in HCC patients and its upregulation is associated with a poor prognosis.

In addition to H4K20me3, H3K9me3 and H3K4me3 levels were also increased in HCC tissues compared with noncancerous liver tissues. Upregulation of H3K9me3 was reported in several cancers, such as gastric cancer [21], colon cancer [22] and HCC [23]. Likewise, H3K4me3 upregulation was demonstrated in esophagus [24] and breast cancers [25]. Patients with esophageal squamous cell carcinoma who had a poor prognosis exhibited high level of H3K9me3, high level of H4K20me3, and low level of H3K36me3 [26]. In early-stage colon cancer patients, low H3K4me3, high H3K9me3 and high H4K20me3 were associated with a good prognosis [27]. Low levels of H3K9me3, H4K20me3, and H3K36me3 in patients with distal common bile duct cancer were associated with poor overall survival and event-free survival [28]. In HCC, increased levels of H3K9me3 and H3K4me3 were associated with short survival and HCC development [7,23]. Previously, we reported that HCC patients had increased oxidative stress compared with the healthy subjects [3, 5]. Our present findings showed that upregulation of H4K20me3, H3K9me3, and H3K4me3 coincided with increased oxidative stress in human HCC. Recently, we demonstrated in bladder cancer cells that chromatin structures were profoundly altered in cells subjected to oxidative stress [12]. Therefore, we hypothesized that ROS might be a cause of histone methylation dysregulation that consequently led to tumor progression in HCC.

Experimentally, we showed that ROS provoked oxidative stress and altered histone methylation in HCC cell lines. In kidney and

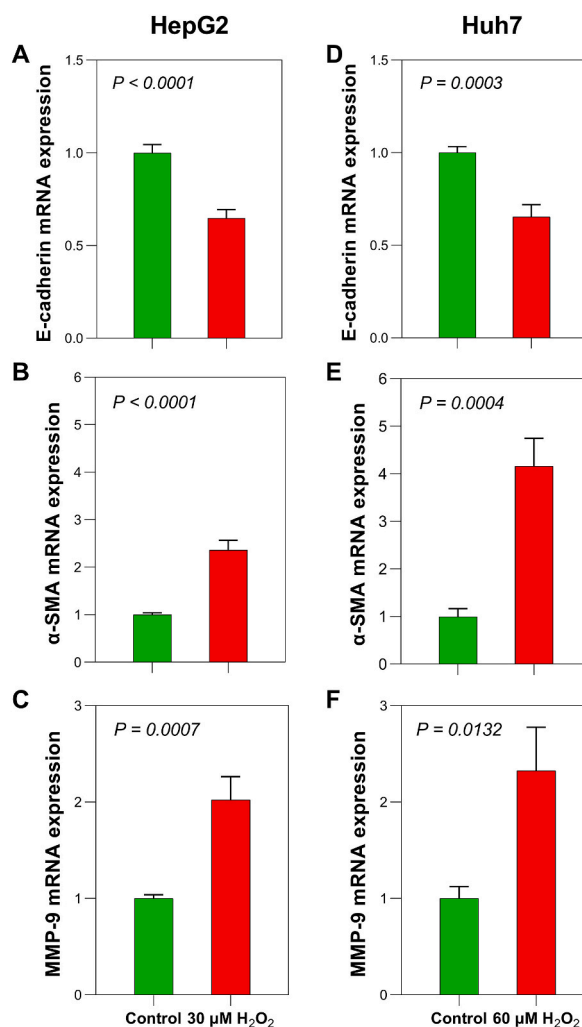


Fig. 6. Induction of EMT by ROS in HepG2 and Huh7 cells. A: mRNA expression of epithelial marker E-cadherin in HepG2 treated with H₂O₂ and untreated control. B: mRNA expression of mesenchymal marker α-SMA in HepG2 treated with H₂O₂ and untreated control. C: mRNA expression of MMP-9 in HepG2 treated with H₂O₂ and untreated control. D: mRNA expression of E-cadherin in Huh7 treated with H₂O₂ and untreated control. E: mRNA expression of α-SMA in Huh7 treated with H₂O₂ and untreated control. F: mRNA expression of MMP-9 in Huh7 treated with H₂O₂ and untreated control. Experiments were done in triplicate. Error bars indicate SEM.

lung cancers, changes in histone modification and expression of histone-modifying enzymes following H₂O₂ exposure were shown to be associated with tumorigenesis and progression [13,14]. Increased Suv420h2 expression was associated with advanced stage of pancreatic cancer [29]. High expression of Suv39h1 and H3K9me3 were associated with development and progression of HCC [23]. In addition, elevated expression of Smyd3 was associated with HCC development in patients with hepatic B virus infection [30]. These lines of evidence suggest that dysregulation of histone modification and histone-modifying enzymes by ROS play vital roles in cancer development.

It is well recognized that ROS induce oxidative stress and promote tumor progression. Recently, we reported that ROS induced cell migration and invasion in bladder cancer cells [31]. However, the role of ROS in tumor progression in HCC is largely unknown. Fundamentally, cancer cells acquire EMT to become more aggressive [32]. Induction of EMT by ROS in cancers is well documented [16,33]. In this study, we asked if ROS promoted HCC progression through EMT. We showed that E-cadherin mRNA was down-regulated in HCC cells following the H₂O₂ treatment. In contrast, α-SMA and MMP-9 transcripts were upregulated in H₂O₂-treated HCC cells. A previous study by Lim et al. demonstrated that ROS activated hypermethylation of E-cadherin promoter via upregulation of Snail [34]. Others showed that ROS (generated through NOX4) activated the TGF-β-induced EMT via Nrf2 signaling pathway [35,36]. MMP-9 plays an essential role in extracellular matrix remodeling and membrane protein cleavage, and it is associated with cancer development. MMP-9 was reported to induce breast cancer metastasis via ROS-dependent MAPK and Akt pathways [37]. Here, we demonstrated that ROS enhanced progressiveness of HCC cells, as seen by increases in colony formation, cell migration, and cell invasion. Although we did not investigate extensively, our findings suggested that ROS increased the aggressive capability of HCC cells

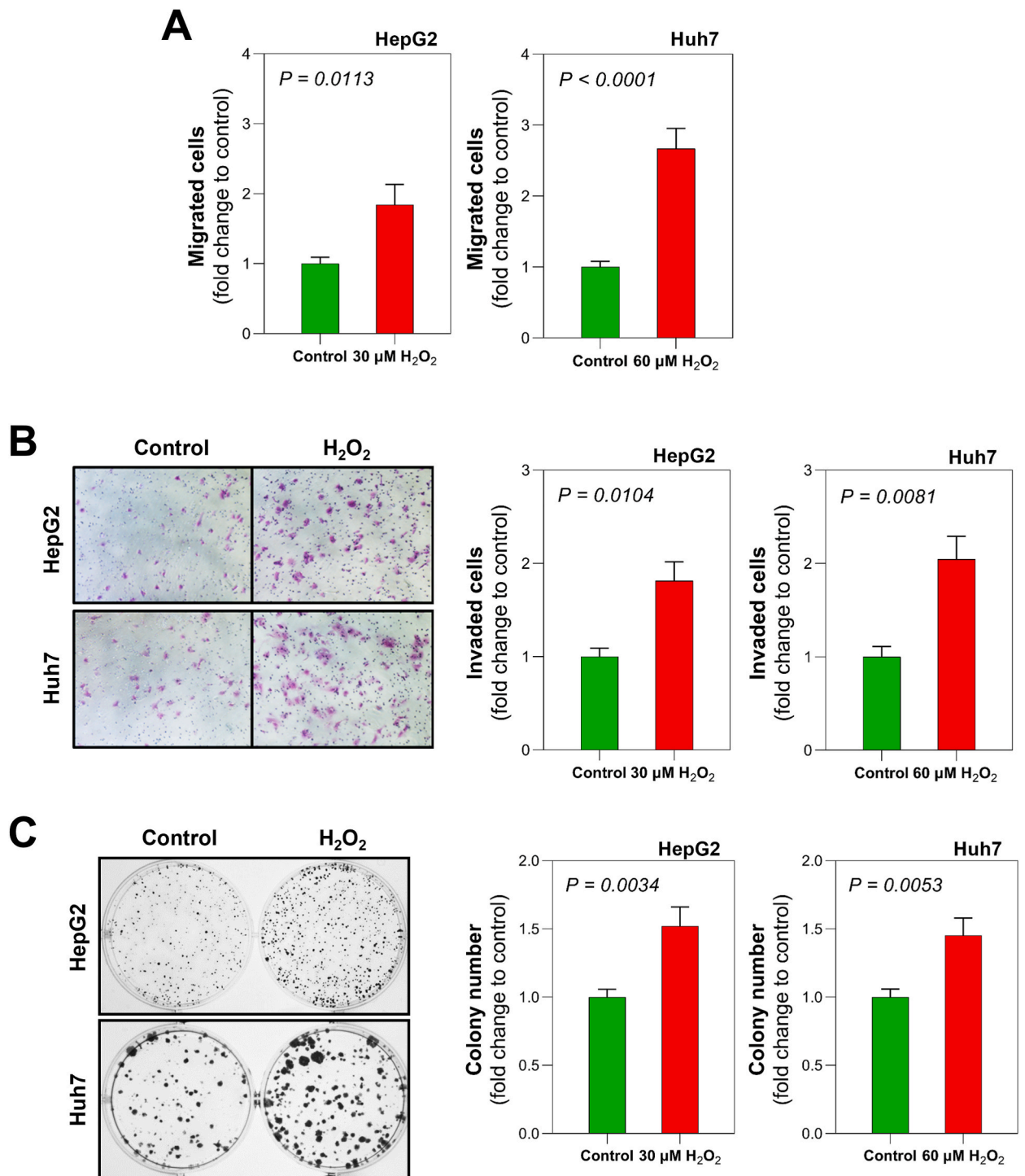


Fig. 7. Tumor aggressiveness induced by ROS in HCC cells. A: Cell migration assay compared between HepG2 and Huh7 cells treated with H_2O_2 and untreated controls. B: Cell invasion assay compared between HepG2 and Huh7 cells treated with H_2O_2 and untreated controls. C: Colony formation assay compared between HepG2 and Huh7 cells treated with H_2O_2 and untreated controls. Experiments were done in triplicate. Error bars indicate SEM.

through EMT acquisition and MMP upregulation.

Recently, Viotti et al. showed that Suv420h2 stimulated EMT through its repressive mark H4K20me3 in pancreatic cancer [29]. In this study, we found that H4K20me3 was upregulated in HCC cells following the H_2O_2 treatment, and it corresponded well with the

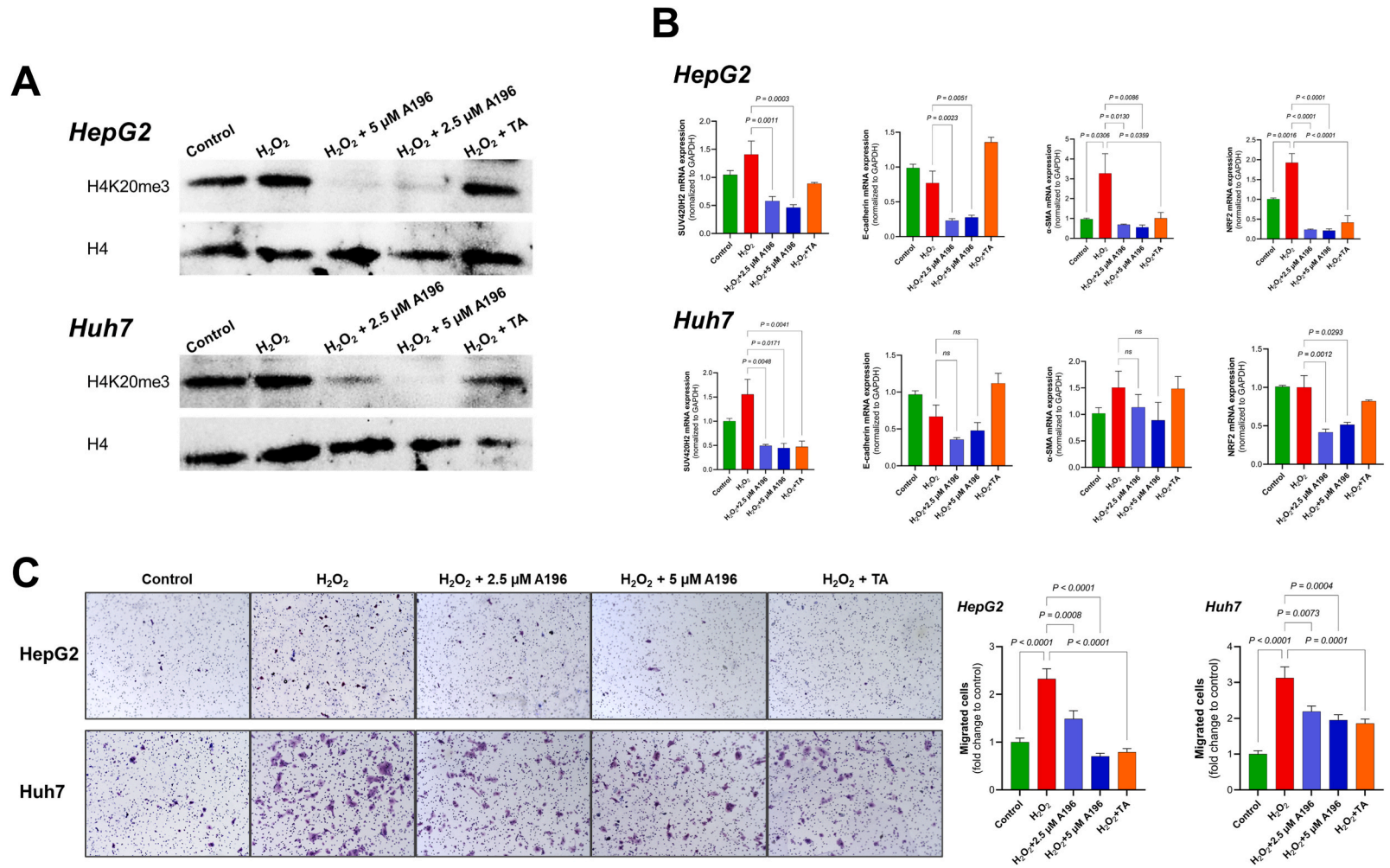


Fig. 8. Inhibition of H4K20me3 formation by Suv420 inhibitor (A196) in H₂O₂-treated HCC cells. A196 and tocopheryl acetate (TA at 300 μM, acted as antioxidant) were co-treated with H₂O₂ in HepG2 and Huh7 cells for 72 h. A: Western blot images showing efficacy of A196 (at 2.5 and 5 μM) in decreasing H4K20me3 level in HepG2 and Huh7 treated with H₂O₂. B: qRT-PCR results showing the effect of A196 and TA on transcript expression of Suv420h2, E-cadherin, α-SMA and Nrf2 in H₂O₂-treated HepG2 and Huh7 cells. C: Cell migration assay showing the inhibition of cell migration by A196 and TA in HepG2 and Huh7 treated with H₂O₂. Experiments were done in duplicate. Error bars indicate SEM. The full non-adjusted blot images are shown in [Supplementary Fig. 6](#).

upregulation of Suv420h2 mRNA (at least in Huh7 cells). We also showed that inhibition of H4K20me3 formation in H₂O₂-treated HCC cells by Suv420 inhibitor could decrease EMT and tumor aggressive phenotype, profoundly observed in HepG2 cells. Taken together, our present findings suggested that upregulation of Suv420h2 by ROS was responsible for an increased formation of H4K20me3 in HCC cells, and the increased H4K20me3 further stimulated EMT and promoted HCC aggressiveness.

Limitations of the study should be mentioned. In this study, HCC cells were treated with a sub-lethal concentration of H₂O₂ for three days. Some epigenetic alterations induced by ROS may require a more extended period, as shown for the 6 months in the study by Mahalingaiah et al. [14]. Protein expression of histone methyltransferases (Suv420h2, Suv39h1, and Smyd3) by Western blot in H₂O₂-treated HCC cells were not investigated. Experiments to validate the effects of H₂O₂ on the levels of histone marks in HCC cells using other pro-oxidant agents were not performed in this study. Since HCC cells already have a certain level of basal oxidative stress, it would be interesting to explore if the basal expression of histone methyltransferases could be reduced by antioxidant intervention. Whether ROS caused changes in chromatin remodeling at EMT-related genes (e.g., inactive chromatin formation at the E-cadherin gene and active chromatin formation at the α -SMA gene) was not investigated in this study, and it should be further explored. For the induction of EMT by H₂O₂, we demonstrated only mRNA expression of EMT markers. Protein expression of EMT markers were not determined.

In conclusion, inactive chromatin (H4K20me3 and H3K9me3) and active chromatin (H3K4me3) were upregulated in human HCC tissues. To our knowledge, this is the first study reporting an increased level of H4K20me3 in human HCC tissues. The elevated hepatic level of H4K20me3 was independently associated with tumor recurrence and poor survival in HCC patients. ROS provoked oxidative stress, increased H4K20me3 formation, induced transcript expression of EMT markers, upregulated MMP-9 mRNA expression, and increased tumor aggressive activities in HCC cells. Suv420 inhibitor decreased H4K20me3 formation, reduced EMT and attenuated tumor aggressive phenotypes in ROS-treated HCC cells. Our findings suggested that the augmentation of EMT and tumor aggressiveness by ROS in HCC was, at least in part, mediated through an increased H4K20me3 formation. Decreasing H4K20me3 formation by histone methyltransferase inhibitor might be a new therapeutic approach to decelerate HCC progression.

Funding

The study was financially supported by the Ratchadapiseksompotch Fund, Faculty of Medicine, Chulalongkorn University (GA65/29) and the Ratchadaphiseksomphot Matching Fund from the Faculty of Medicine, Chulalongkorn University (to C.B.). S.P. was awarded the Thailand Research Fund under the Royal Golden Jubilee Ph.D. Scholarship (PHD/0030/2558) and the 90th Anniversary of Chulalongkorn University Scholarship. N.H. was supported by the Ratchadaphiseksomphot Matching Fund from the Faculty of Medicine, Chulalongkorn University.

Ethics statement

This study was reviewed and approved by the Ethics Committee, Faculty of Medicine, Chulalongkorn University, Bangkok, Thailand, with the approval number: COA No. 846/2021 and IRB No. 289/62. All participants provided informed consent to participate in the study.

Data availability statement

Data will be made available on request.

CRedit authorship contribution statement

Suchittra Phoyen: Writing – review & editing, Visualization, Validation, Methodology, Investigation. **Anapat Sanpavat:** Writing – review & editing, Visualization, Methodology. **Chakriwong Ma-on:** Writing – review & editing, Methodology. **Ulrike Stein:** Writing – review & editing, Supervision, Resources, Conceptualization. **Nattiya Hirankarn:** Writing – review & editing, Resources. **Pisit Tangkijvanich:** Writing – review & editing, Resources. **Depicha Jindatip:** Writing – review & editing, Methodology. **Patcharawalai Whongsiri:** Writing – review & editing, Visualization, Methodology, Investigation. **Chanchai Boonla:** Writing – review & editing, Writing – original draft, Supervision, Resources, Project administration, Funding acquisition, Formal analysis, Conceptualization.

Declaration of competing interest

The authors declare the following financial interests/personal relationships which may be considered as potential competing interests: Suchittra Phoyen reports financial support was provided by Thailand Research Fund under the Royal Golden Jubilee Ph.D. Scholarship. Chanchai Boonla reports a relationship with Chulalongkorn University, Faculty of Medicine that includes: employment and funding grants.

Acknowledgements

Thanks to Pimkanya More-krong, and lab members of CBLAB806 for excellent assistance. Also, thanks to Jiraphorn Issara-amphorn and Jiradej Makjaroen for their kind support.

Appendix A. Supplementary data

Supplementary data to this article can be found online at <https://doi.org/10.1016/j.heliyon.2023.e22589>.

References

- [1] Z. Zhao, A. Shilatfard, Epigenetic modifications of histones in cancer, *Genome Biol.* 20 (1) (2019) 245.
- [2] M.G. Fernandez-Barrena, M. Archederra, L. Colyn, C. Berasain, M.A. Avila, Epigenetics in hepatocellular carcinoma development and therapy: the tip of the iceberg, *JHEP Rep* 2 (6) (2020), 100167.
- [3] C. Ma-On, A. Sanpavat, P. Whongsiri, S. Suwannasin, N. Hirankarn, P. Tangkijvanich, et al., Oxidative stress indicated by elevated expression of Nrf2 and 8-OHdG promotes hepatocellular carcinoma progression, *Med. Oncol.* 34 (4) (2017) 57.
- [4] M. Marra, I.M. Sordelli, A. Lombardi, M. Lamberti, L. Tarantino, A. Giudice, et al., Molecular targets and oxidative stress biomarkers in hepatocellular carcinoma: an overview, *J. Transl. Med.* 9 (2011) 171.
- [5] P. Pongpairaj, P. Whongsiri, S. Suwannasin, A. Khlaiphungsins, P. Tangkijvanich, C. Boonla, Increased oxidative stress and RUNX3 hypermethylation in patients with hepatitis B virus-associated hepatocellular carcinoma (HCC) and induction of RUNX3 hypermethylation by reactive oxygen species in HCC cells, *Asian Pac J Cancer Prev* 16 (13) (2015) 5343–5348.
- [6] S. Reuter, S.C. Gupta, M.M. Chaturvedi, B.B. Aggarwal, Oxidative stress, inflammation, and cancer: how are they linked? *Free Radic. Biol. Med.* 49 (11) (2010) 1603–1616.
- [7] C. He, J. Xu, J. Zhang, D. Xie, H. Ye, Z. Xiao, et al., High expression of trimethylated histone H3 lysine 4 is associated with poor prognosis in hepatocellular carcinoma, *Hum. Pathol.* 43 (9) (2012) 1425–1435.
- [8] Y. Qian, Y. Li, C. Zheng, T. Lu, R. Sun, Y. Mao, et al., High methylation levels of histone H3 lysine 9 associated with activation of hypoxia-inducible factor 1alpha (HIF-1alpha) predict patients' worse prognosis in human hepatocellular carcinomas, *Cancer Genet* 245 (2020) 17–26.
- [9] M.Y. Cai, J.H. Hou, H.L. Rao, R.Z. Luo, M. Li, X.Q. Pei, et al., High expression of H3K27me3 in human hepatocellular carcinomas correlates closely with vascular invasion and predicts worse prognosis in patients, *Mol. Med.* 17 (1–2) (2011) 12–20.
- [10] A. Hayashi, N. Yamauchi, J. Shibahara, H. Kimura, T. Morikawa, S. Ishikawa, et al., Concurrent activation of acetylation and tri-methylation of H3K27 in a subset of hepatocellular carcinoma with aggressive behavior, *PLoS One* 9 (3) (2014), e91330.
- [11] Y. Niu, T.L. DesMarais, Z. Tong, Y. Yao, M. Costa, Oxidative stress alters global histone modification and DNA methylation, *Free Radic. Biol. Med.* 82 (2015) 22–28.
- [12] P. Whongsiri, C. Pimratana, U. Wijitsettakul, A. Sanpavat, D. Jindatip, M.J. Hoffmann, et al., Oxidative stress and LINE-1 reactivation in bladder cancer are epigenetically linked through active chromatin formation, *Free Radic. Biol. Med.* 134 (2019) 419–428.
- [13] F.M. Moodie, J.A. Marwick, C.S. Anderson, P. Szulakowski, S.K. Biswas, M.R. Bauter, et al., Oxidative stress and cigarette smoke alter chromatin remodeling but differentially regulate NF-kappaB activation and proinflammatory cytokine release in alveolar epithelial cells, *Faseb. J.* 18 (15) (2004) 1897–1899.
- [14] P.K. Mahalingaiah, L. Ponnusamy, K.P. Singh, Oxidative stress-induced epigenetic changes associated with malignant transformation of human kidney epithelial cells, *Oncotarget* 8 (7) (2017) 11127–11143.
- [15] P. Whongsiri, S. Phoyen, C. Boonla, Oxidative stress in urothelial carcinogenesis: measurements of protein carbonylation and intracellular production of reactive oxygen species, *Urothelial Carcinoma: Springer* (2018) 109–117.
- [16] J. Jiang, K. Wang, Y. Chen, H. Chen, E.C. Nice, C. Huang, Redox regulation in tumor cell epithelial-mesenchymal transition: molecular basis and therapeutic strategy, *Signal Transduct. Targeted Ther.* 2 (2017), 17036.
- [17] S.Y. Lee, M.K. Ju, H.M. Jeon, Y.J. Lee, C.H. Kim, H.G. Park, et al., Reactive oxygen species induce epithelial-mesenchymal transition, glycolytic switch, and mitochondrial repression through the Dlx2/Snai1 signaling pathways in MCF7 cells, *Mol. Med. Rep.* 20 (3) (2019) 2339–2346.
- [18] A. Sepsa, G. Levidou, A. Gargalionis, C. Adamopoulos, A. Spyropoulou, G. Dalagiorgou, et al., Emerging role of linker histone variant H1x as a biomarker with prognostic value in astrocytic gliomas. A multivariate analysis including trimethylation of H3K9 and H4K20, *PLoS One* 10 (1) (2015), e0115101.
- [19] A. Van Den Broeck, E. Brambilla, D. Moro-Sibilot, S. Lantuejoul, C. Brambilla, B. Eymin, et al., Loss of histone H4K20 trimethylation occurs in preneoplasia and influences prognosis of non-small cell lung cancer, *Clin. Cancer Res.* 14 (22) (2008) 7237–7245.
- [20] E. Ozgur, M. Keskin, E.E. Yoruker, S. Holdenrieder, U. Gezer, Plasma histone H4 and H4K20 trimethylation levels differ between colon cancer and precancerous polyps, *In Vivo* 33 (5) (2019) 1653–1658.
- [21] J. Xu, W. Wang, X. Wang, L. Zhang, P. Huang, Expression of SIRT1, H3K9me3, H3K9ac and E-cadherin and its correlations with clinicopathological characteristics in gastric cancer patients, *Int. J. Clin. Exp. Med.* 9 (9) (2016) 17219–17231.
- [22] Y. Yokoyama, M. Hieda, Y. Nishioka, A. Matsumoto, S. Higashi, H. Kimura, et al., Cancer-associated upregulation of histone H3 lysine 9 trimethylation promotes cell motility in vitro and drives tumor formation in vivo, *Cancer Sci.* 104 (7) (2013) 889–895.
- [23] T. Chiba, T. Saito, K. Yuki, Y. Zen, S. Koide, N. Kanogawa, et al., Histone lysine methyltransferase SUV39H1 is a potent target for epigenetic therapy of hepatocellular carcinoma, *Int. J. Cancer* 136 (2) (2015) 289–298.
- [24] X.D. Ye, B.Q. Qiu, D. Xiong, X. Pei, N. Jie, H. Xu, et al., High level of H3K4 tri-methylation modification predicts poor prognosis in esophageal cancer, *J. Cancer* 11 (11) (2020) 3256–3263.
- [25] L. Berger, T. Kolben, S. Meister, T.M. Kolben, E. Schmoedel, D. Mayr, et al., Expression of H3K4me3 and H3K9ac in breast cancer, *J. Cancer Res. Clin. Oncol.* 146 (8) (2020) 2017–2027.
- [26] M. Zhou, Y. Li, S. Lin, Y. Chen, Y. Qian, Z. Zhao, et al., H3K9me3, H3K36me3, and H4K20me3 expression correlates with patient outcome in esophageal squamous cell carcinoma as epigenetic markers, *Dig. Dis. Sci.* 64 (8) (2019) 2147–2157.
- [27] A. Benard, I.J. Goossens-Beumer, A.Q. van Hoesel, W. de Graaf, H. Horati, H. Putter, et al., Histone trimethylation at H3K4, H3K9 and H4K20 correlates with patient survival and tumor recurrence in early-stage colon cancer, *BMC Cancer* 14 (2014) 531.
- [28] H.G. Kim, J.Y. Sung, K. Na, S.W. Kim, Low H3K9me3 expression is associated with poor prognosis in patients with distal common bile duct cancer, *In Vivo* 34 (6) (2020) 3619–3626.
- [29] M. Viotti, C. Wilson, M. McClelland, H. Koeppen, B. Haley, S. Jhunjhunwala, et al., SUV420H2 is an epigenetic regulator of epithelial/mesenchymal states in pancreatic cancer, *J. Cell Biol.* 217 (2) (2018) 763–777.
- [30] M.T. Binh, N.X. Hoan, D.P. Giang, H.V. Tong, C.T. Bock, H. Wedemeyer, et al., Upregulation of SMYD3 and SMYD3 VNTR 3/3 polymorphism increase the risk of hepatocellular carcinoma, *Sci. Rep.* 10 (1) (2020) 2797.
- [31] P. Whongsiri, C. Pimratana, U. Wijitsettakul, D. Jindatip, A. Sanpavat, W.A. Schulz, et al., LINE-1 ORF1 protein is up-regulated by reactive oxygen species and associated with bladder urothelial carcinoma progression, *Cancer Genomics Proteomics* 15 (2) (2018) 143–151.
- [32] P. Storz, Reactive oxygen species in tumor progression, *Front. Biosci.* 10 (2005) 1881–1896.
- [33] S. Cannito, E. Novo, L.V. di Bonzo, C. Busletta, S. Colombatto, M. Parola, Epithelial-mesenchymal transition: from molecular mechanisms, redox regulation to implications in human health and disease, *Antioxid Redox Signal* 12 (12) (2010) 1383–1430.
- [34] S.O. Lim, J.M. Gu, M.S. Kim, H.S. Kim, Y.N. Park, C.K. Park, et al., Epigenetic changes induced by reactive oxygen species in hepatocellular carcinoma: methylation of the E-cadherin promoter, *Gastroenterology* 135 (6) (2008) 2128–2140, 2140 e2121–2128.

- [35] R. Hiraga, M. Kato, S. Miyagawa, T. Kamata, Nox4-derived ROS signaling contributes to TGF-beta-induced epithelial-mesenchymal transition in pancreatic cancer cells, *Anticancer Res.* 33 (10) (2013) 4431–4438.
- [36] D. Ryu, J.H. Lee, M.K. Kwak, NRF2 level is negatively correlated with TGF-beta1-induced lung cancer motility and migration via NOX4-ROS signaling, *Arch Pharm. Res. (Seoul)* 43 (12) (2020) 1297–1310.
- [37] G.H. Lee, S.W. Jin, S.J. Kim, T.H. Pham, J.H. Choi, H.G. Jeong, Tetrabromobisphenol A induces MMP-9 expression via NADPH oxidase and the activation of ROS, MAPK, and Akt pathways in human breast cancer MCF-7 cells, *Toxicol. Res.* 35 (1) (2019) 93–101.